Numerical simulation of the width and angle of the rotor blade on the air flow rate of a 350 kW air-cooled eddy current dynamometer

by Nazaruddin Sinaga

Submission date: 10-Jan-2020 09:49AM (UTC+0700)
Submission ID: 1240514655
File name: 2.pdf (12.27M)
Word count: 4699
Character count: 23245

Numerical simulation of the width and angle of the rotor blade on the air flow rate of a 350 kW air-cooled eddy current dynamometer

Numerical simulation of the width and angle of the rotor blade on the air flow rate of a 350 kW air-cooled eddy current dynamometer

Nazaruddin Sinaga[1,*]

1. Introduction

Eddy currents are electric currents induced in a conductor when exposed to a changing magnetic field, due to the relative motion or variation of the magnetic source and conductor with time. It can cause a circulating flow of electrons, or current, within the body of the conductor. These eddies have inductance and thus induce magnetic fields. Like conventional friction brakes, eddy current brakes are responsible for slowing down an object, such as rotating machinery, a moving train, or even a roller coaster. Another use of this eddy current is to produce lift force on the train (magnetic levitation) or other equipment such as electromagnetic (attractive force) suspension (levitation) and electrodynamic (repulsive) suspension [1]. In the application of electric motors and electric generators, the presence of eddy currents is avoided because it is an irreversible loss, which in turn converts into heat. In this study, eddy currents were made to produce as much as possible to be used as energy absorbers in dynamometers.

The use of a dynamometer to measure the torque and power of the engine has long been known, especially in the automotive machinery industry. Eddy current dynamometer is a type of dynamometer that is widely used in the automotive world, both as a dynamometer and as a braking system (retarder). Some of these advantages are: independent of wheel support, no contact, no wear or tear, no noise or smell, adjustable brake force, high brake forces at high speeds, it uses electromagnetic force and not friction, can be activated at will via an electrical signal, low maintenance, and lightweight. The disadvantages include: braking force diminishes as speed diminishes with no ability to hold the load in

position at a standstill, it cannot be used at low-speed vehicles, electromagnetic brakes are used with ordinary mechanical brakes. Nowadays, electromagnetic brakes are used only for safety purpose [2].

Eddy current dynamometer works according to Faraday's law of electromagnetic induction. According to this law, whenever a conductor cuts magnetic lines of forces, an electromotive force, is induced in the conductor, the magnitude of which is proportional to the strength of the magnetic field and the speed of the conductor. If the conductor is a disc, there will be circulatory currents, i.e., eddy currents in the disc. According to Lenz's law, the direction of the current is in such a way as to oppose the cause, i.e., movement of the disc. The eddy current brake consists of two parts, a stationary magnetic field system, and a solid rotating part, which include a metal disc. During braking, the metal disc is exposed to a magnetic field from an electromagnet, generating eddy currents in the disc. The magnetic interaction between the applied field and the eddy currents slow down the rotating disc. Figure1 illustrated an eddy current braking system principle [3].

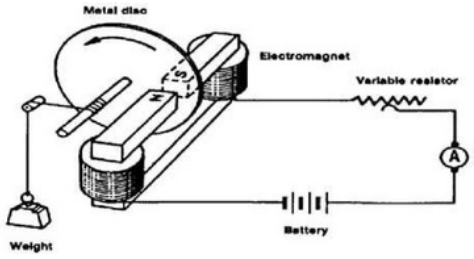

Figure 1. The principle of eddy current braking operation

As explained earlier, besides being a dynamometer, the effect of this eddy current can also be used to braking a rotor, which is called a retarder. Brakes like this are excellent to use as a brake device for a vehicle because these brakes do not experience wear like the brake disk or drum brakes. Even though there is no wear surface, this retarder will receive heat due to braking, so the best cooling system is needed. If the cooling system is inadequate, then the stator and rotor surface will experience a high increase in temperature so that the braking power capacity decreases significantly [4]. The use of dynamometers in laboratories and vehicle workshops is necessary, not only to measure torque and power but also used to measure the brake thermal efficiency (BTE) and the brake specific fuel consumption (BSFC). If this tool is not owned by a workshop, it is not possible to know what the torque capacity and power of the vehicle are being serviced, as well as BSFC and BTE [5]. Dynamometers must also be owned by automobile dealers to know exactly how much torque and power of the vehicle to be sold, or that has undergone repairs or an engine tune-up.

To run an energy efficiency program and an environmentally friendly transportation system, a dynamometer is also needed to determine the fuel economy, in units of km/liter, and the emissions of a vehicle, in units of gr/km. In measuring these two quantities, the vehicle is run on a chassis dynamometer by following a driving scenario called the Driving Cycle. To be able to follow this driving cycle, the vehicle must be loaded by a dynamometer. Until now, there are almost no workshops or vehicle dealers in Indonesia that use dynamometer for the purposes mentioned above. This is because the price of a dynamometer is still relatively high, especially by small-scale workshops, because until now there has been no factory that makes dynamometers in the country.

To be able to make an eddy current dynamometer is indeed not easy, especially by its usage requirements, which are limited by the function of the rotor speed to torque and power, commonly called a dynamometer envelope. Currently, eddy current dynamometers are divided into two types, namely air-cooled and water-cooled. Air-cooled dynamometers have a more straightforward

construction than water-cooled ones, so the price is relatively lower compared to water-cooled ones. However, the cooling capacity of the air-cooled eddy current dynamometers is much lower than the water-cooled eddy current dynamometer. This cooling capacity plays a vital role in determining the measuring capacity of the dynamometer after operating in a steady state. Liu et al. [6], and Prasetiyo and Sinaga [7] showed that a decrease in torque measurement capacity could decrease by 70% by using an air-cooled. On the other side, the use of water cooling only reduces the measurement capacity by around 15% [8]. Therefore, efforts need to be made to increase the cooling capacity of the air-cooled eddy current dynamometers, for example by design optimization using artificial neural networks [9, 10]

A water-cooled eddy current dynamometer usually consists of a stator, which produces a magnetic field, and one or two rotors producing eddy currents and at the same time as a cooler, as shown in figure 2. To be able to design a compact dynamometer, the ability to optimize all parameters involved with torque and power capacity. To do this, optimization is complicated because it involves many parameters [11-13]. Optimization involving the process of making a prototype certainly requires quite expensive costs. Therefore, the researchers are currently making efforts using parameter optimization from the simulation results using computational methods. The calculation using computational fluid dynamics software is now very much done because the results are quite close to the measurement results. With the help of this CFD software, calculations can be done quickly. However, the accuracy of the results of these theoretical calculations must first be justified so that the results have low uncertainty. When a precise calculation model has been obtained, the effect of various design parameters from the dynamometer can be searched quickly. This research was conducted in order to obtain a calculation model that can be used to perform the optimal design of the air-cooled eddy current dynamometer.

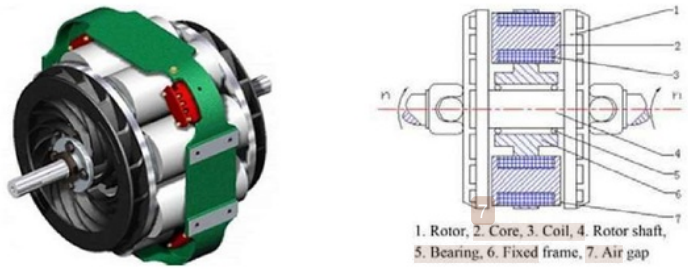

Figure 2. Construction of air-cooled eddy current dynamometer and its components

From the descriptions above, it can be concluded that design of cooling part of air-cooled eddy current dynamometer plays an essential role since the effect of temperature rise will dramatically drop the capacity of power and torque measurement. The air flow rate of the rotor will undoubtedly affect the temperature of the rotor surface and the stator dynamometer. Since the flow and heat transfer mechanism is very complicated and involves many parameters affecting cooling capacity, it is essential to study the phenomena before designing a dynamometer. The study aims to investigate the effect of the rotor blade design to the air flow rate of the rotor of a 350 kW air-cooled eddy current dynamometer, which has the rotor diameter of 520 mm and the number of the blade is 16. In this paper, the impacts of the rotor blade width, as well as inlet and outlet angle, were analyzed against the air flow rate in some speed of the rotor the dynamometer. The finite volume method, facilitated by ANSYS FLUENT software, is used to solve the problem.

2. Methodology

In this study, the method used is a computational approach, namely the finite volume method. This is a method that is widely used in solving fluid flow and heat transfer problems numerically. In the finite volume method, unknown variables are explained using a specific point on the nodal points. Broadly speaking, the necessary steps for solving problems using the finite volume method are as follows: estimating the value of unknown flow variables using a simple function; make a discretization equation by entering the estimation into the general equation of flow, and then doing mathematical manipulation; and finally solve the algebraic equation of the problem at hand [14]. Currently, there is quite a several computational fluid dynamic software that can be used to solve flow problems and heat transfer. In this study, ANSYS FLUENT® software is used. One of the advantages of the software is its complete literature and is very widely used in scientific. Besides, this software also has complete features.

2.1 Geometry and Flow Conditions

In the present calculation, the rotor plate outer diameter is 520 mm, the inner diameter of the front rotor plate is 220 mm, the inner diameter of the rear rotor plate is 460 mm, the number of blades is 16 pieces, and the rotor material is made of St 60 steel. The blade width is 50, 60, 70 and 90 mm, with the rotor blade entry angle are 55°, 58°, 61°, 64°, 67°, 70° and 73°, while the blade exit angle is 17°, 20°, 23°, 26°, 29°, and 32°. The geometry of the dynamometer rotor is shown in figure 3.

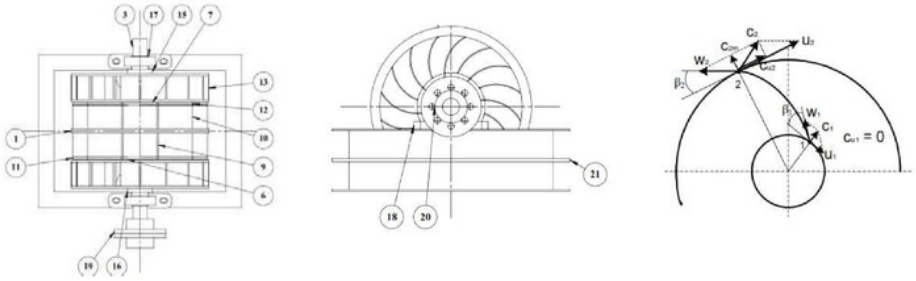

Figure 3. The geometry of the dynamometer: (a) above view; (b) right view; (c) inlet and outlet angle of the rotor blade

2.2 Problem Description

The problem involves modeling the steady-state flow of air through a rotor running at 1500 rpm. There are 16 blade rows in the rotor. To simplify the CFD calculation, the flow is modeled only through double blade rows and uses rotationally periodic boundary conditions on the boundaries between the blade rows. The governing equations are cast in a Single Reference Frame moving at the speed of the rotor. Air is treated as an ideal gas with constant values of specific heat, thermal conductivity, and dynamic viscosity. The schematic of a single blade row and the complete rotor, repeating a single blade row 16 times, are shown in figure 4.

2.3 Model and Materials

As a first step in the modeling in ANSYS FLUENT, we have to set up the general model as follows: enable the density-based, steady-state solver and retain the default values for the other parameters. The second step is to enable the Spalart-Allmaras turbulence model, and retain the default values for the other parameters. This turbulence model is an excellent and economical choice for mildly complex boundary-layer flows in turbomachinery. The next step is to set the density of air to ideal-gas. The

ideal gas model will automatically enable the solution of the energy equation. For simplicity, we will keep the other fluid properties at their default constant values, though they could be made the function of temperature if desired.

(a) (b) (c)

Figure 4. (a) calculated geometry; (b) full rotor geometry; (c) meshing on the domain geometry

2.4 Boundary Conditions

In figure 5, a cell zone conditions setting is shown in the blade area, which is then given a rotational speed with a specific value in the rotational velocity, for example, 1500 rpm. In this inlet area, the pressure is 1000 Pa gauge, and the initial gauge pressure is 1000 Pa, while the turbulent viscosity ratio is 10. The outlet condition is a pressure outlet of 1000 Pa, and the turbulent viscosity ratio backflow is 10. Figure 5 also shown the boundary conditions at the hub, shaft, shroud-b, and shroud-d areas, where the wall is a moving wall, relative to adjacent cell zone with the rotational axis is X = 1, and rotational speed is zero. For wall boundary conditions of blade1-p, blade1 -s, blade2-p, and blade2-s, the settings are the same as before.

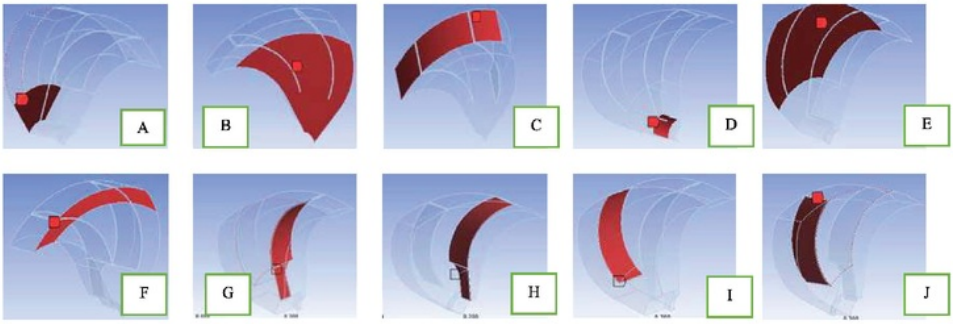

Figure 5. Boundary conditions at inlet-B, D, outlet, and wall

2.5 Solver Discretization, Controls, and Monitors

Retain the default solution methods for flow under solve methods, and set the turbulence equation to second order upwind. Activate the pseudo transient method then retain the default solution controls under solving controls. For the residual convergence, set the convergence criterion for continuity to 1e-4. Create three surface monitors as follows: mass flow rate at the inlet, the mass flow rate at the outlet, and mass-averaged total pressure at the outlet.

Tabel 1. The boundary condition at inlet and outlet

Surface	Boundary Condition	Label
Inlet-D	Intake Fan	A
Inlet-B	Intake Fan	B
Outlet	Exhaust Fan	C
Hub	wall	D
Shroud-D	wall	E
Shroud-B	wall	F
Blade1-P	wall	H
Blade1-S	wall	I
Blade2-P	wall	J

2.6 Solver Discretization, Controls, and Monitors

Retain the default solution methods for flow under solve methods, and set the turbulence equation to second order upwind. Activate the pseudo transient method then retain the default solution controls under solving controls. For the residual convergence, set the convergence criterion for continuity to 1e-4. Create three surface monitors as follows: mass flow rate at the inlet, the mass flow rate at the outlet, and mass-averaged total pressure at the outlet.

3. Results and Discussion

Figure 6 shows the iteration process by observing the residual value and mass flow rate on the outlet side. Figure (a) shows that the iteration process runs quite well towards convergence. In this calculation, the number of cells used is 104,000, which has been tested by the grid-independence test. Although in this study, the residual value is limited to 1e-4, from the residual diagram, it can be seen that up to 3300th the iteration reaches a minimum residual value of 1e-5. This is not very influential on the results of the calculation of mass flow rates, as seen on figure (b). From this value, it can be seen that the calculation has been almost constant since the 1500th iteration. By using a PC with a Pentium-7 processor and 12 GB of memory, the calculation can be completed in 10 minutes.

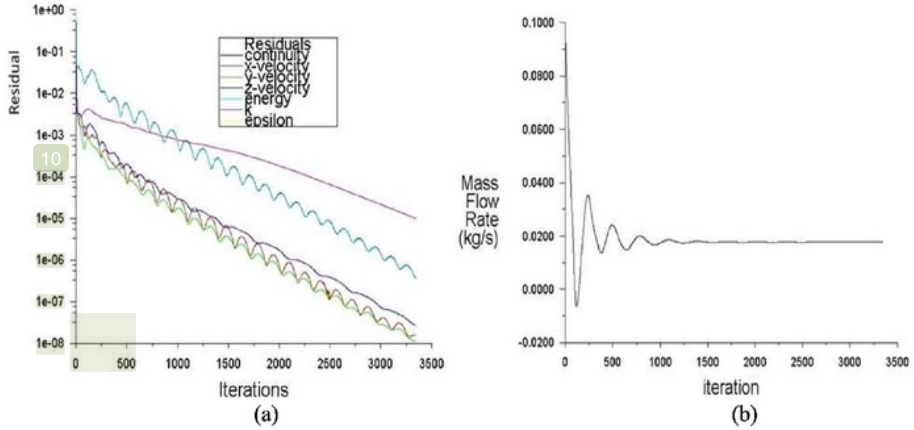

Figure 6. Residual iteration (a) and iteration of mass flow rate (b) for controlling calculation

3.1 Particle Pathline

To ascertain the direction of flow in the calculation results, figure 7 shows the path lines of the fluid particles in the middle area of the rotor, x = 4.5 mm. From the two pictures, it is clear that the flow is sucked in through the front and rear inlet holes, and is ejected through the outlet side. It is also seen that the movement of fluid flow is quite smooth, and only a few swirls occur. From this pathline, the fluid movements can also be learned from the inlet to the outlet. This observation can give intuition to improve the geometry of the rotor dynamometer so that the resulting geometry is compact but has a more significant flow rate. With an increase in the flow rate, the cooling capacity becomes higher, and ultimately increases the torque capacity and power of the dynamometer.

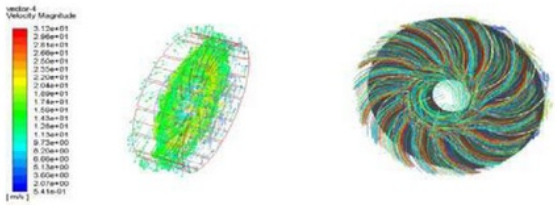

Figure 7. Particle pathline in the middle of the rotor, x = 4.5 mm

3.2 Velocity Contour

Figure 8 shows the tangential, radial, and total velocity contours. It can be seen that the tangential velocity is higher in the area leading to the outlet, while the radial velocity value is relatively more significant in the area of the central part of the rotor. The resultant of these two speeds is the total speed, which is shown in the rightmost image (c). For the rotor cooling process, the dominant speed in conducting convection heat transfer is radial velocity. Based on figure 8 (b), it can be estimated that the area that is effective in heat transfer is the area between the inlet and outlet sides of the rotor. To get a useful heat transfer geometry, it is necessary to find a design that results in a more uniform distribution of radial velocity, starting from the inlet to the outlet side. From figure 7 and 8 it can be said that the flow is reasonable and as expected.

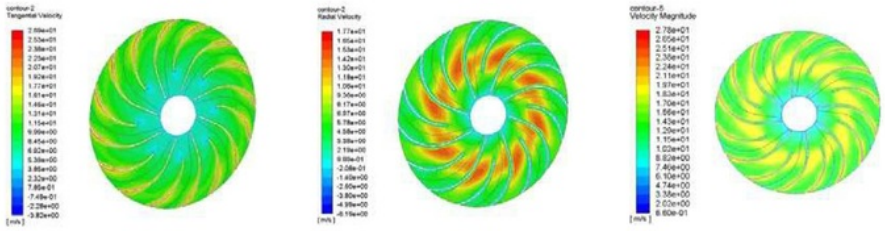

(a) (b) (c)

Figure 8. Tangential, radial and velocity magnitude in the middle of the rotor, x = 4.5 mm

3.3 Pressure Contour

Figure 9 shows the static, dynamic, and total pressure contours. The total pressure is the sum of static and dynamic pressure. The dynamic pressure contour is similar to the speed contour. This is quite clear because dynamic pressure is a pressure that arises due to speed or kinetic energy. The static pressure contour is the opposite of the speed contour. This can be explained using the Bernoulli equation, where the line with a high velocity has low pressure. Therefore the speed and pressure contours generated from the calculation are reasonable and as expected. The value of static pressure on the side of the inlet and outlet is also by the value of the boundary conditions given at the two places, that is 1000 Pa. Observation of the path line, velocity, and pressure contour give the conclusion that the results of this numerical calculation are good enough. The particle pathline, velocity and pressure contour are agree well with the one calculated in Fluent Tutorial [14].

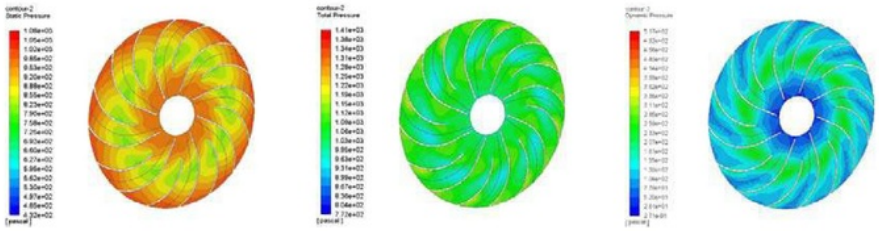

(c) (b) (c)

Figure 9. Static, total and dynamic pressure in the middle of the rotor, x = 4.5 mm

3.4 Effect of the Blade Width

In figure 10 (a), the calculation results of the effect of blade width on the flow rate at the inlet and exit of the dynamometer are shown. It can be seen that the flow rate through the outlet is the same as the sum of the flow rate through the front inlet and the rear inlet. The flow rate through the rear inlet is much smaller than the flow rate through the front inlet. This is because the rear inlet surface area is smaller than the front inlet surface area, while the pressure is almost the same, that is atmospheric pressure. It can also be seen that the blade width is very influential on flow discharge. If a regression equation is made for all three lines, an equation in the form of a parabolic equation is obtained. This indicates that there is an optimum value of the blade width, which gives the highest flow rate. In the simulation carried out in this study, the width of the blade that gives the maximum flow rate is 90 mm.

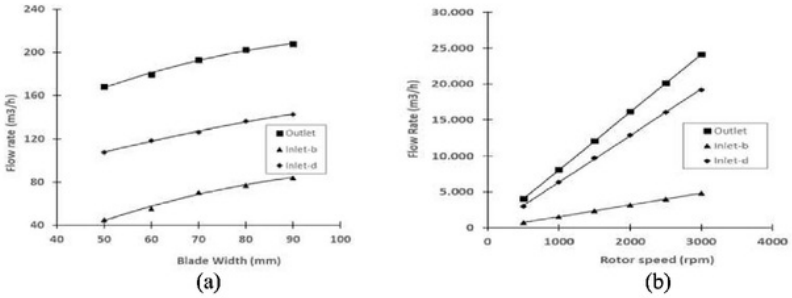

(a) (b)

Figure 10. Effect of blade width at 1500 rpm (a) and rotor speed (b) on the air flow rate

3.5 Effect of the Rotor Speed

Figure 10 (b) shows the effect of rotor speed on flow discharge at the front and rear inlet and outlet for optimal blade geometry. In this case, the blade width is 90 mm, blade inlet angle 73 degrees and the blade outlet angle is 26 degrees. It can be seen that the effect of the rotor speed on the flow rate is linear, that is, the higher the rotor speed, the higher the flow rate. It can be seen that the lowest line gradient is at the flow discharge that enters the rear inlet side. Therefore it can be concluded that the effect of the rotor speed is more significant in the front inlet side. In this study, the maximum flow rate that passes through the outlet side is around 24,200 m3/h at a rotor speed of 3000 rpm. To be able to increase the flow rate at the rear inlet side and the outlet side can be done by enlarging the rear inlet diameter. These results also in accordance with the results of measurements carried out by Fauzi [15].

3.6 Effect of the Blade Inlet Angle

The calculation of the effect of the inlet angle on the flow rate at the front inlet, rear inlet, and outlet side is shown in figure 11 (a). As in the previous explanation, the flow rate at the rear inlet side is smaller than the flow rate through the front inlet side. Unlike the previous pictures, the effect of the inlet angle on the front inlet is different in shape compared to the rear inlet side. It can be seen that with increasing the inlet angle, the flow discharge at the front inlet side will tend to reduce the flow rate. However, the effect of the inlet angle on the flow discharge at the front inlet side is not as strong as the effect on the rear inlet side. Therefore, the flow rate at the outlet side will increase with increasing blade inlet angle. It can also be seen that there is an optimal inlet angle value that gives the highest flow discharge. In this study, the angle is 73 degrees.

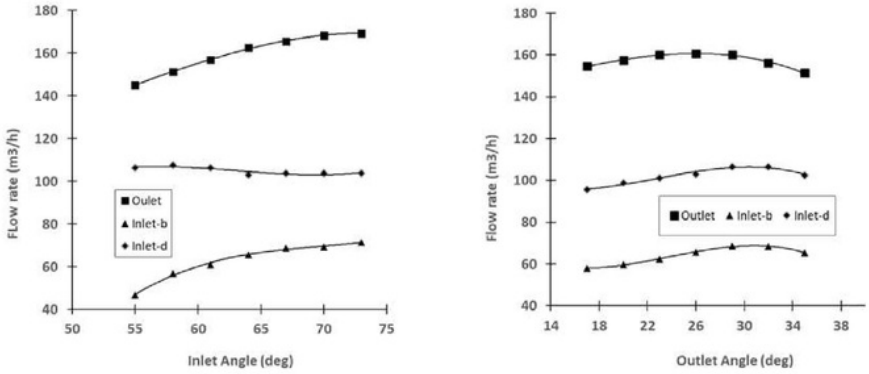

(a) (b)

Figure 11. Effect of blade inlet (a) and outlet (b) angle on the air flow rate at 1500 rpm

3.7 Effect of the Blade Outlet Angle

Figure 11 (b) shows the calculation of the effect of the outlet blade angle on the flow rate at the front and rear inlet as well as the outlet. It can be seen that the influence of the blade angle is in the form of the quadratic polynomial equation, wherein the calculated angle range, there is a value that gives maximum discharge. In this study, the blade outlet angle which gives maximum discharge is at 26 degrees. Based on the discussion before, it can be concluded that the blade geometry which provides maximum discharge is at 90 mm blade width, 73° inlet angle, and 26° blade outlet angle.

4. Conclusion

Based on the results of the study, the geometry parameters, namely blade width, blade inlet angle and blade outlet angle have a significant effect on the flow rate produced by the rotor as well as the rotating speed and direction of the blade rotation. Therefore, to get the best design, it is necessary to optimize these parameters. It was found that the higher the speed of the rotor, the higher the air flow rate. It is also found that the addition of the blade width will increase the air flow rate so it could increase the heat transfer rate and the torque and power capacity of the dynamometer. Moreover, there is an optimum value of both the inlet and outlet blade angle which give the maximum amount the air flow rate. The optimum inlet angle is 64°, while the optimum outlet angle is 26° and the blade width is 90 mm. In general, it can be concluded that there are optimum geometric parameters of the dynamometer design that will give the best performance of the dynamometer. This paper provides a useful method for matching and designing the cooling part of the air-cooled eddy current dynamometer.

The speed and direction of the rotor also have a significant effect on the air flow rate generated by the rotor, where the backward type blade produces a higher flow rate than the forward type. The influence of the rotor speed on the flow discharge indicates that with the greater rotational speed, the higher the value of the discharge produced. At 3000 rpm, the forward facing blade generates a discharge of 20,700 m3/h, while at 500 rpm generates a discharge of 1325 m3/h. At 3000 rpm, the backward facing blade generates a discharge of 24,200 m3/h, while at 500 rpm generates a discharge of 1650 m3/h. Therefore, cooling using backward blades would be more effective than the forward blade.

Numerical simulation of the width and angle of the rotor blade on the air flow rate of a 350 kW air-cooled eddy current dynamometer

ORIGINALITY REPORT

10%	8%	5%	0%
SIMILARITY INDEX	INTERNET SOURCES	PUBLICATIONS	STUDENT PAPERS

PRIMARY SOURCES

1	www.slideshare.net Internet Source	5%
2	An, Xiang Bi, Da Wei Li, Hu Wang, and Long Wang. "The Modal Analysis of the Rotor of Electric Eddy Current Dynamometer Based on ADAMS", Applied Mechanics and Materials, 2012. Publication	1%
3	www.cfd-online.com Internet Source	1%
4	S. Hall, M. Cooke, A. El-Hamouz, A.J. Kowalski. "Droplet break-up by in-line Silverson rotor–stator mixer", Chemical Engineering Science, 2011 Publication	1%
5	etd.adm.unipi.it Internet Source	1%
	www.scribd.com	

6	Internet Source	<1%
7	Jin, Fu, Jian Jun Sun, and Hong Bin Yu. "Design of Control System of Eddy Current Retarder Based on BP Neural Network PID Controller", Applied Mechanics and Materials, 2014. Publication	<1%
8	indtechies.blogspot.co.uk Internet Source	<1%
9	forums.randi.org Internet Source	<1%
10	www.readbag.com Internet Source	<1%
11	www.mdpi.com Internet Source	<1%
12	Tsutomu Adachi, Naohiro Sugita, Yousuke Yamada. "Study on the Performance of a Sirocco Fan (Optimum Design of Blade Shape)", International Journal of Rotating Machinery, 2001 Publication	<1%
13	S. Lee, Y. Chu, W.H. Chung, S.J. Lee et al. "AC Loss Characteristics of the KSTAR CSMC Estimated by Pulse Test", IEEE Transactions on Applied Superconductivity, 2006 Publication	<1%

14	S.C Bhattacharya, A.H.Md Mizanur Rahman Siddique, Hoang-Luong Pham. "A study on wood gasification for low-tar gas production", Energy, 1999 Publication	<1%
15	Viktoriia Miltykh, Mykola Sotnyk. "Chapter 33 Numerical Study of Outlet Blade Angle Effect on Impeller Characteristics of Double Entry Centrifugal Pump", Springer Science and Business Media LLC, 2019 Publication	<1%

Exclude quotes	Off	Exclude matches	Off
Exclude bibliography	Off		

Numerical simulation of the width and angle of the rotor blade on the air flow rate of a 350 kW air-cooled eddy current dynamometer

GRADEMARK REPORT

FINAL GRADE

/0

GENERAL COMMENTS

Instructor

PAGE 1

PAGE 2

PAGE 3

PAGE 4

PAGE 5

PAGE 6

PAGE 7

PAGE 8

PAGE 9

PAGE 10

PAGE 11